ELSEVIER

Nuclear Instruments and Methods in Physics Research A 430 (1999) 559–569

NUCLEAR INSTRUMENTS & METHODS IN PHYSICS RESEARCH Section A

www.elsevier.nl/locate/nima

Modeling quantum noise of phosphors used in medical X-ray imaging detectors

N. Kalivas[a], I. Kandarakis[b], D. Cavouras[b], L. Costaridou[a], C.D. Nomicos[c], G. Panayiotakis[a,*]

[a]*Department of Medical Physics, School of Medicine, University of Patras, 265 00 Patras, Greece*

[b]*Department of Medical Instrumentation Technology, Technological Educational Institution of Athens, Ag. Spyridonos Street, Aigaleo, Athens, Greece*

[c]*Department of Electronics, Technological Educational Institution of Athens,Ag. Spyridonos Street, Aigaleo, Athens, Greece*

Received 12 August 1998; received in revised form 21 December 1998

Abstract

The noise properties of the granular phosphor screens, which are utilized in X-ray imaging detectors, are studied in terms of the quantum noise transfer function (QNTF). An analytical model, taking into account the effect of K-characteristic X-rays reabsorption within the phosphor material and the optical properties of the phosphor, was developed. The optical properties of the phosphor material required by the model were obtained from literature, except for the optical diffusion length (σ) that was determined by data fitting and was found to be 26 cm^2/g. The deviation between theoretical and experimental data is σ depended. Specifically for $\sigma = 26$ cm^2/g and $\sigma = 25$ cm^2/g the respective deviations between experimental and predicted results were 0.698% and -1.597%. However for relative differences in σ more than 15% from the value 26 cm^2/g, the corresponding deviations exceed by 6 times the value of 0.698%. The model was tested via comparison to experimental results obtained by a set of Y_2O_3:Eu^{3+} phosphor screens prepared by sedimentation. The model may be used to evaluate the effect of screen thickness and irradiation geometry on quantum noise of phosphor materials for transmission and reflection mode.

Keywords: Phosphor detector; Quantum noise; K-characteristic; Model

1. Introduction

Phosphor materials usually in the form of screens are employed in the majority of medical X-ray imaging detectors. The intrinsic physical properties of these materials strongly affect the image detector transfer characteristics, such as the modulation transfer function (MTF) and noise power spectrum (NPS). Noise limits the quantity and clarity of diagnostic information that an image detector can display [1]. In radiographic systems, either conventional (screen-film) or digital (phosphors coupled with CCD arrays etc.), the noise associated with the phosphor material (screen noise) is the main component of total image noise [1,2].

Phosphor screen noise can be distinguished in the following two components: (i) Quantum mottle, mainly produced by the statistical nature of the spatial fluctuations of the absorbed X-ray quanta.

* Correspondence address. Tel.: + 30-61-996113; fax: + 30-61-992496.

E-mail address: panayiot@upatras.gr (G. Panayiotakis)

0168-9002/99/$ - see front matter
PII: S0168-9002(99)00232-6

This may be the dominant noise component, especially in the low and medium spatial frequency region, below 20 cm^{-1} [3]. The spatial frequency range contained in quantum mottle patterns is depended upon phosphor characteristics (X-ray absorption and optical properties). Furthermore, above 60 cm^{-1} it should be compared with the noise spectra of the other noise sources, since X-ray quantum noise decreases relatively faster with frequency [3]. (ii) Screen structure mottle, due to phosphor grains and their spatial distribution. This component may be considered negligible, due to advanced manufacturing techniques [2]. Noise is evaluated in terms, of either the noise power spectrum (NPS) (also called the Wiener spectrum), or in terms of the noise transfer function [1–7].

In this study an analytical model of the quantum noise of granular phosphors is presented. Quantum noise is studied through a quantum noise transfer function (QNTF). This QNTF considers: (i) the X-ray energy spectrum, (ii) the X-ray absorption efficiency, corrected for the effect of production and reabsorption of K characteristic X-rays when the X-ray energy spectrum encompasses the K-edge of the high Z element of the phosphor, (iii) the optical properties (absorption and scatter of light photons) of the phosphor material and (iv) the thickness of the screen. Previously published work on modeling quantum noise is either based on analytical modeling which does not take into account the K-absorption edge effects, or on Monte Carlo methods [5,8–11]. However, the present Monte Carlo methods either do not take into account granular phosphors through NPS and QNTF, or the effect of phosphor thickness in light escape or X-ray spectrum and phosphor material optical properties. The quantum noise of granular phosphors predicted by the model was validated against experimental results obtained with a set of laboratory prepared Y_2O_3:Eu^{3+} screens.

2. Materials and methods

2.1. Noise model

If the X-rays incident on the phosphor have energy above the K-edge of the high Z element of the phosphor material, K-characteristic X-rays will be produced. When this happens, the total energy deposited in the phosphor is the sum of: (i) the energy deposited directly by the incident X-rays, where the fraction of the energy given for the generation of K-characteristics is not included, (ii) the energy that is deposited in the phosphor by K-characteristic X-rays. These energy deposition processes are not affected by each other, in the sense that by the first process the energy required for the production of K-characteristics X-rays has been excluded, while in the second process the amount of energy deposited in the phosphor by the K X-rays is not affected by the energy directly deposited by the incident X-rays. Furthermore, these two energy deposition processes can be described separately for all energies above the K-edge of the high Z element of any phosphor material [9,10,12,13]. Thus, the total noise associated with an X-rayed phosphor screen can be expressed as the quadrature sum of three signal variances corresponding to: (i) the direct absorption of the incident X-rays (σ_Q^2), (ii) the absorption of K-characteristic radiation (σ_K^2), and (iii) the screen granular structure (σ_g^2). Therefore the output variance (σ_{Total}^2), giving the total screen noise is expressed as

$$\sigma_{Total}^2 = \sigma_Q^2 + \sigma_K^2 + \sigma_g^2. \quad (1)$$

If the incident X-ray spectrum does not encompass the K-absorption edge of the high Z element of the phosphor, the second term in Eq. (1) is zero.

2.1.1. Direct absorption of incident X-rays

Consider an X-ray fluence distribution $f(E)$, with energy between E and $E + dE$ incident on a phosphor screen of thickness T. The screen is considered to consist of N thin layers of thickness Δt [6,14,16]. A fraction of the incident quanta will interact at various depths in the screen and a part of their energy will be deposited within the phosphor material. This absorption process follows Poisson distribution (see appendix). The number of X-ray quanta of energy E absorbed in a layer of thickness Δt, at depth t, in the screen is denoted by $q(f(E), t)$, where,

$$q(f(E), t) = f(E)e^{-\mu_{en}t}\mu_{en}\Delta t, \quad (2)$$

where μ_{en} is the total mass energy absorption coefficient of the phosphor material. It does not

account for characteristic photon production and reabsorption within the material [12,13]. The absorbed X-ray energy is partially converted into light photons. This process is characterized by the intrinsic gain of the screen $m(E)$, which is defined as the number of light photons that are produced within the phosphor per absorbed X-ray of energy E. $m(E)$ is calculated by

$$m(E) = n_C E/E_\lambda, \tag{3}$$

where n_C is the intrinsic conversion efficiency of the screen [14,15] expressing the fraction of absorbed X-ray energy that is converted into light and E_λ is the energy of the optical photons. Hence, the total number of light quanta that are produced within this layer equals to $q(f(E), t)m(E)$.

The light quanta are emitted in all directions, but only a fraction of these quanta denoted $G(0, t)$ escapes to the output. This is because of losses due to scattering, absorption, and reflection at the output interface. If one photon of energy E is absorbed in depth t in the phosphor, then $m(E)G(0, t)$ light quanta escape and spread to the output. If the spatial distribution of $m(E)G(0, t)$ is Fourier transformed and divided by $m(E)$, then a function $G(u, t)$ is obtained where $G(u, t) = G(0, t)\mathrm{MTF}(u, t)$ [16]. $\mathrm{MTF}(u, t)$ is the modulation transfer function of a thin phosphor layer at depth t and u is the spatial frequency. If $q(f(E), t)$ absorbed X-ray photons are considered, then the mean number, $M(E, t)$, of the light quanta escaping to the output equals to:

$$M(E, t) = q(f(E), t)m(E)G(0, t). \tag{4}$$

This number can be expressed as a function of spatial frequency:

$$M(u, E, t) = q(f(E), t)m(E)G(u, t). \tag{5}$$

In the case of front screen configuration setup (transmission mode), where the light emitted by the surface of the phosphor screen opposite to the X-ray source is considered, $G(u, t)$ is given by [6,15–18]

$$G(u, t) = G(0, t)\mathrm{MTF}(u, t) = \frac{\tau\rho_i[(b + \tau\rho_o)e^{-bt} + (b - \tau\rho_o)e^{-bt}]}{(b + \tau\rho_o)(b + \tau\rho_i)e^{bT} - (b - \tau\rho_o)(b - \tau\rho_i)e^{-bT}}; \tag{6a}$$

where MTF is the modulation transfer function of the phosphor layer at depth t, b is an optical parameter given by

$$b = \sqrt{(\sigma^2 + 4\pi^2u^2)}, \tag{6b}$$

σ is the reciprocal diffusion length given by the formula:

$$\sigma = \sqrt{a(a + 2s)}, \tag{6c}$$

where a and s are the optical absorption and scattering coefficients. τ is the inverse relaxation length given by

$$\tau = \frac{\sigma}{\beta} \quad \text{and} \quad \beta = \sqrt{[a/(a + 2s)]} \tag{6d}$$

both σ and τ characterize optical absorption and scattering and

$$\rho_i = (1 - r_i)(1 + r_i)^{-1}, \tag{6e}$$

where r_i is the reflectivity of the inner surface of the screen at either the input, 0, or the output, 1, interfaces. Relation (6a) has been derived by Swank [17] under the following assumptions: (i) there are no discontinuities in the properties of the screen, (ii) solutions are sought for points far from the source and (iii) the probability of absorption is small compared with the probability of scattering.

In the case of back screen configuration setup (reflection mode), where the light emitted by the surface of the phosphor screen facing the X-ray source is considered, Eq. (6a) is changed to [14,17,19]

$$G(u, t) = \frac{\tau\rho_i[(b + \tau\rho_o)e^{b(t-T)} + (b - \tau\rho_o)e^{-b(t-T)}]}{(b + \tau\rho_o)(b + \tau\rho_i)e^{bT} - (b - \tau\rho_o)(b - \tau\rho_i)e^{-bT}}; \tag{7}$$

The variance in the number of output light photons $M(u, E, t)$ is a measure of quantum noise. Since the process of X-ray energy absorption follows Poisson distribution (see appendix) the variance of the output signal equals [20]

$$\mathrm{var}[M(u, E, t)] = q(f(E), t)[m(E)G(u, t)]^2. \tag{8}$$

The product $m(E)G(u, t)$ represents the number of light photons, generated per absorbed X-ray of

energy E at a thin layer, that reach the screen output.

If the total screen thickness T is considered, then the variance is given by integrating over t as

$$\text{var}[M(u,E)] = m^2(E)\int_0^T q(f(E),t)[G(u,t)]^2\,\mathrm{d}t = \text{QNPS}(u,E). \quad (9)$$

Relation (9) defines the QNPS for monoenergetic X-ray beams. For polyenergetic X-ray beams QNPS is obtained by integrating over the X-ray spectrum:

$$\text{QNPS}(u) = \int_0^{kV_p} m^2(E)\int_0^T q(f(E),t)[G(u,t)]^2\mathrm{d}t\,\mathrm{d}E, \quad (10)$$

where kV_p is the X-ray tube voltage, which is numerically equal to the maximum X-ray spectral energy (in keV).

The quantum noise transfer function QNTF is defined as the square root of the noise power spectrum at zero spatial frequency [6]:

$$\text{QNTF}^2(u) = \frac{\text{QNPS}(u)}{\text{QNPS}(0)}. \quad (11)$$

2.1.2. Escape and absorption of characteristic X-rays

If the energy spectrum of the incident X-ray beam encompasses the K-edge of the high Z element of the phosphor, X-ray characteristic radiation is generated. This phenomenon degrades the transfer characteristics of the image detector [20], due to re-absorption of characteristic photons far from the point of primary interaction.

If an X-ray interaction occurs at depth $t = i\Delta t$, where $i = 1,2,\ldots,N$, in the phosphor material and if the X-ray energy is above the K-absorption edge of the high Z element of the phosphor material, characteristic radiation will be created. The energy carried by the K-photons is given by [12]

$$E_{\text{Ki}} = \Phi(E,i\Delta t)P_{\text{K}}\omega_{\text{K}}E_{\text{K},\alpha\beta} \quad (12)$$

where, $\Phi(E,i\Delta t)$ is the fraction of the fluence of the X-ray photons of energy E that interact with the layer at depth $i\Delta t$, (i.e. $\Phi(E,i\Delta t) = f(E)\lfloor \mathrm{e}^{-\mu_{\text{tot}}i\Delta t} - \mathrm{e}^{-\mu_{\text{tot}}(i+1)\Delta t}\rfloor$, where μ_{tot} is the total mass attenuation coefficient for energy E), ω_{K} is the fluorescence yield [12], $E_{\text{K},\alpha\beta}$ is the mean energy of K-characteristic photons of the phosphor. P_{K} is given by

$$P_{\text{K}} = \frac{\mu_{\text{pe}}/\rho}{\mu_{\text{tot}}/\rho}\,w_z f_{\text{K}} I_{\text{K}}, \quad (13)$$

where w_z is the fractional weight of the high Z element of the phosphor, (μ_{pe}/ρ) is the photoelectric mass attenuation coefficient at energy E, f_{K} is the K-shell contribution to the photoelectric effect for the high Z element of the phosphor, I_{K} is the relative frequency of K-photons production [12,13].

K-characteristic photons are isotropically emitted from the point of their creation within a solid angle 4π. If the solid angle is divided into $2m$ solid angle elements denoted by $\Delta\Omega_{\text{r}}$ then

$$\Delta\Omega_r = 2\pi[\cos(r-1)\Delta\theta - \cos(r\Delta\theta)], \quad r = 1,2,\ldots,2m, \quad (14)$$

where $\Delta\Theta$ is the polar angle, which is equal to $\pi/2m$. Thus, the energy carried away by K photons per solid angle element equals to $(\Delta\Omega_{\text{r}}/4\pi)E_{\text{Ki}}$.

The K X-rays will interact in the screen and a part of their energy will be absorbed. K X-rays will interact at different depths t. If a layer of thickness Δt at depth t in the screen is considered, the energy of K X-rays that is absorbed in it, is due to the contribution of characteristic photons emerging from different depths. In Fig. 1 a two dimensional schematic representation of the K X-rays interactions within the phosphor is demonstrated.

The energy per solid angle element carried away by the K-photons emerging from the layer at depth $t = i\Delta t$ and absorbed by a layer at $t = j\Delta t$ equals to

$$Y_{r,i,j}(E,E_{\text{Ki}},\Delta\Omega_{\text{r}}) = \frac{\Delta\Omega_{\text{r}}}{4\pi}E_{\text{Ki}}\mathrm{e}^{-\frac{\mu_{\text{enK}}|j-i|\Delta t}{\cos(r\Delta\theta)}}(1-\mathrm{e}^{-\mu_{\text{enK}}\Delta t/\cos(r\Delta\theta)}), \quad j = 1,2,\ldots,N, \quad i = 1,2,\ldots,N, \quad (15)$$

where, the factor in front of the parenthesis accounts for the total energy per solid angle element of the K-characteristic photons incident on the

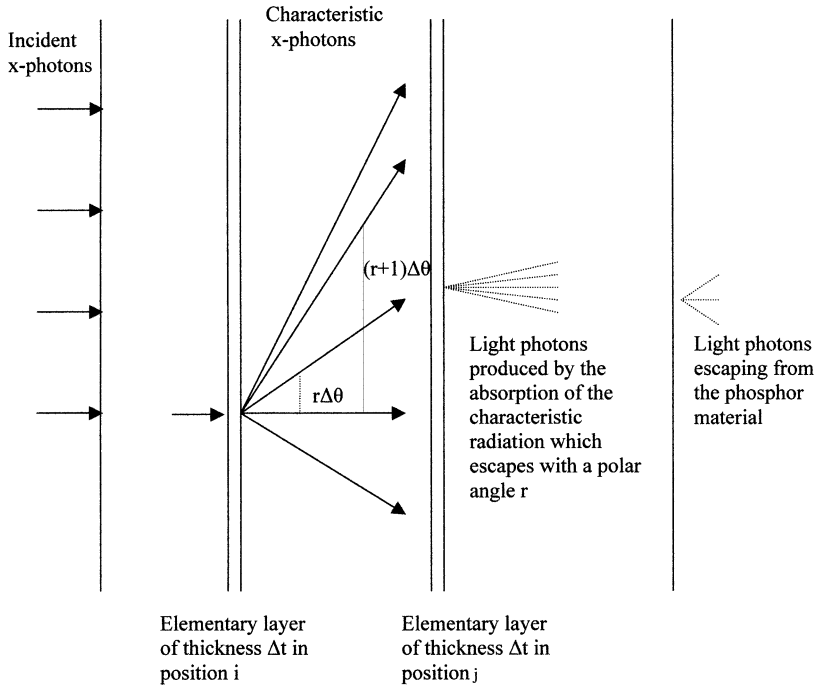

Fig. 1. A schematic representation of the main steps considered in the production of light photons within an elementary layer Δt at position j of the phosphor, due to the generation of K characteristic X-rays in an elementary layer Δt at position i.

layer at position j and μ_{enK} stands for the total mass energy absorption coefficient of the phosphor for energy $E_{\mathrm{K}\alpha,\beta}$. Eq. (15) is actually providing the intensity of the K-characteristic photons that is absorbed in a layer positioned at j. By dividing Eq. (15) by the energy $E_{\mathrm{K}\alpha,\beta}$ of the K-photon, the number of K-photons absorbed in this layer can be obtained, thus

$$Y'_{r,i,j}(E,\Delta\Omega_{\mathrm{r}}) = \frac{Y_{r,i,j}(E,E_{\mathrm{Ki}},\Delta\Omega_{\mathrm{r}})}{E_{\mathrm{K}\alpha,\beta}}. \tag{16}$$

Considering $2m$ solid angle elements and N thin screen layers, then the total number of characteristic photons that are absorbed within the layer positioned at $j\Delta t$ equals to

$$q_j(E) = \sum_{i=1}^{N-1}\sum_{r=1}^{m} Y'_{r,i,j}(E,\Delta\Omega_{\mathrm{r}}). \tag{17}$$

The absorbed X-ray energy is partially converted into light photons. The total number of light quanta produced from all the interacting X-ray quanta absorbed in that elementary layer is $m(E_{\mathrm{K}})q_j(E)$. Light quanta are emitted in all directions, but only a fraction of these quanta escape to the output because of scattering, absorption, and reflection at the output interface. This fraction, denoted by $M_{jK}(E)$ equals

$$M_{jK}(E) = m(E_{\mathrm{K}})q_j(E)G_{\mathrm{K}}(0, j\Delta t) \tag{18}$$

or considering the spatial frequency dependence of M_{K}:

$$M_{j\mathrm{K}}(u, E) = m(E_K)q_j(E)G_{\mathrm{K}}(u, j\Delta t). \tag{19}$$

The corresponding variance of M_{K} equals to

$$\mathrm{var}(M_{j\mathrm{K}}) = q_j(E)[m(E_{\mathrm{K}})G(u, j\Delta t)]^2 \tag{20}$$

which is analogous to Eq. (8). By considering contributions from all layers, the variance or the quantum noise power spectrum ($\mathrm{QNPS_K}$), for the

characteristic photons absorption, is given as

$$\mathrm{QNPS_K}(u, E) = \sum_{j=1}^{N} q_j(E)[m(E_K)G(u, j\Delta t)]^2. \quad (21)$$

If the X-ray energy spectrum irradiating the screen is taken into account, Eq. (21) is integrated over the energy range, giving

$$\mathrm{QNPS_K}(u) = \int_0^{kVp} m^2(E_K) \sum_{j=1}^{N} q_j(E)(G(u, j\Delta t))^2 \mathrm{d}E. \quad (22)$$

The quantum noise transfer function, corrected for the effect of K-characteristic photons $\mathrm{QNTF_{cor}}$ can then be derived by the following equation:

$$\mathrm{QNTF^2cor}(u) = \frac{\mathrm{QNPS}(u) + \mathrm{QNPS_K}(u)}{\mathrm{QNPS}(0) + \mathrm{QNPS_K}(0)}. \quad (23)$$

2.2. Implementation

In order to validate the model, a set of Y_2O_3:Eu^{3+} screens were prepared by sedimentation on fused silica substrates with coating thicknesses of 32, 72 and 112 mg/cm^2. The phosphor material was supplied in powder form with grain size of about 7 μm by Riedel de Haen-Lumilux Ltd (Code Number 54009). This type of phosphor may be suitable for digital imaging, since its emission spectrum is compatible with the sensitivity spectrum of CCD arrays [14].

The noise measurement was performed by bringing the phosphor screens in close contact with a film (AGFA Scopix LT2B) sensitive to their emission spectrum (red). The above configuration was irradiated with a mammography X-ray unit (molybdenum target tube and 30 kVp X-ray spectrum filtered by a 51 mm plexiglass). The exposure was 6.32 mR. This value is among the lowest values reported for NPS measurements in 30 kVp [21–23]. Furthermore the sedimentation technique, used for screen preparation, results in uniform distribution of phosphor grains. Thus, the contribution of the screen structure noise to NPS for the above mentioned exposure value can be considered small as compared to the quantum noise pattern, which is expected to dominate even beyond 70 cm^{-1}.

The irradiation geometry for the validation of the model comprised transmission mode measurements. The exposed films were scanned with a 1200×1200 dpi, 12 bit scanner (MICROTEC Scanmaker II SP) with a corresponding pixel size of about 21 μm. A corresponding scanning slit of 21 μm width and 27.3 mm length was utilized. For the image noise analysis, a uniformly exposed area of 1300×1300 pixels was selected.

Noise power spectrum was evaluated as the Fourier transform of the autocorrelation function [1,2,4], taking into account the transfer characteristics of the scanner. The noise components of the experimental chain, besides the screen noise, were the noise due to the scanner and the noise due to the radiographic film. These components were subtracted as follows. The film was exposed to a homogeneous light source, matching the screen emission spectrum (red) by means of a photographic camera [2]. Since the film noise depends upon exposure, the cameras shutter and diaphragm were kept open until the same optical density as in the case of the irradiated screen film was achieved. The film was then processed and digitized. Hence, the only noise components on the image were those of the film and the digitizer. The corresponding Wiener spectrum was calculated as described before and subtracted from the total. Therefore, the Wiener spectrum of the screen noise was obtained.

The X-ray attenuation coefficients used in Eqs. (10), (14) and (16) were derived by the following formula, which is valid for compound mixtures:

$$\left(\frac{\mu_X}{\rho}\right)_E = \sum_k w_k \left(\frac{\mu_X}{\rho}\right)_{k,E}, \quad (24)$$

where k denotes the element in consideration, μ_X is the required coefficient for a given energy and w_i is its fractional weight. The Mo X-ray spectrum utilized in relations (10) and (22), was described and calculated using a previously published theoretical model [24].

The K-edge of the high Z element of the phosphor Y ($Z = 39$) is at 17.02 keV, while the values for its fluorescent parameters are, $f_K = 0.856$, the average energy $E_{K\alpha,\beta} = 15.2$ keV, while I_K is unity [11]. The value of the fluorescent yield for yttrium is 0.71 [25].

3. Results and discussion

Fig. 2 shows the QNTF data calculated using relation (23) for three Y_2O_3:Eu screens of 32, 72, and 112 mg/cm^2, determined at 30 kVp with molybdenum spectrum X-rays. Curves represent results obtained by fitting Eq. (22) to experimental data, using the Levenberg–Marquard method [26]. The correlation between the experimental data and the theoretical model is demonstrated in Fig. 3. It is observed that for the thin screen of 32 mg/cm^2 the coincidence between measured and calculated values is poorer especially in high frequencies. This occurs because thin screens may not fully comply with the assumptions (i) and (ii) presented in the materials and method section, necessary to derive relations (6). That is: (i) The thin screen may not be perfectly homogeneous (i.e. presents discontinuities), due to lower uniformity in the phosphor grain deposition. (ii) The distance between the point of light creation within the phosphor mass and the screen output may not be adequate for the majority of the phosphor layers in thin screens. This fact can also explain the poor correlation between experimental and theoretical results for the 72 mg/cm^2 phosphor for high spatial frequencies, since a number of phosphor layers considered in Eqs. (9) and (21) is near the screen output.

During the fitting procedure the values of parameters η_C, β, ρ_i were kept constant; their values were obtained from literature [13]. This was justified, since β and ρ had been previously experimentally determined and n_C mainly depends on intrinsic phosphor properties and the type of activator. Thus, only parameter σ was allowed to vary.

Best curve fitting was achieved for $\sigma = 26$ cm^2/g. This value accounts for exposure conditions of a Mo spectrum at 30 kVp, where the K X-rays contribution in energy deposition in the phosphor by using Eqs. (11)–(15) is around 15%.

The value of $\sigma = 26$ cm^2/g is compared with a value already reported in literature which was $\sigma = 25$ cm^2/g. This value however has been obtained under different exposure conditions of 50–200 kVp tungsten spectrum X-rays. Under

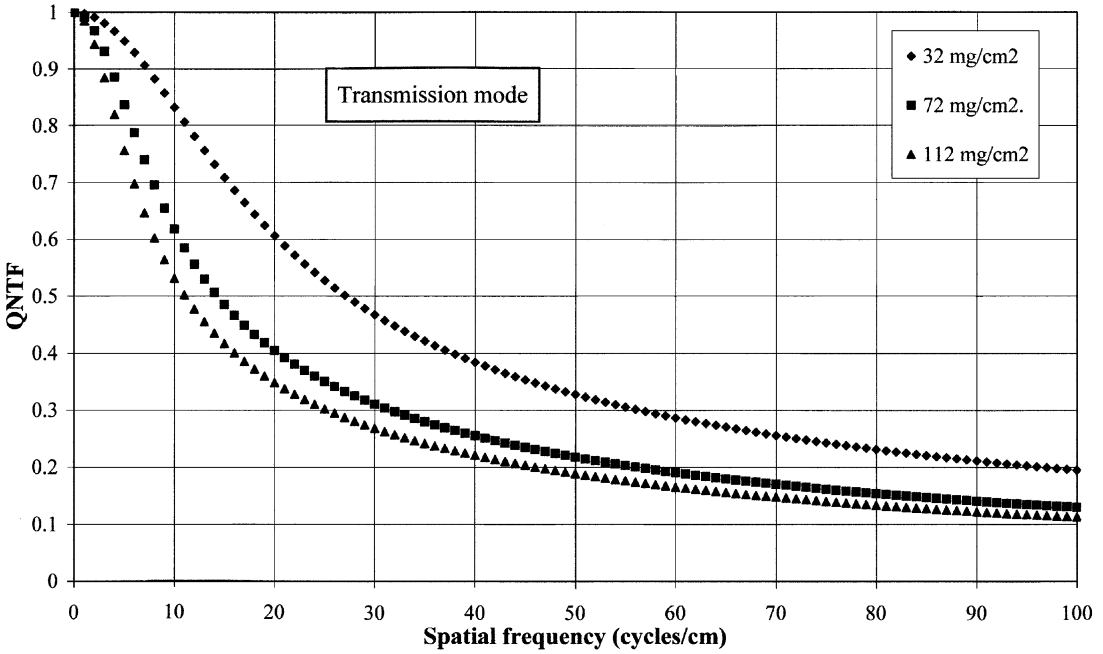

Fig. 2. Model predicted QNTF taking into account the K characteristics X-rays of three Y_2O_3:Eu^{3+} phosphors, corresponding to coating thicknesses of 32, 72 and 112 mg/cm^2, in transmission mode.

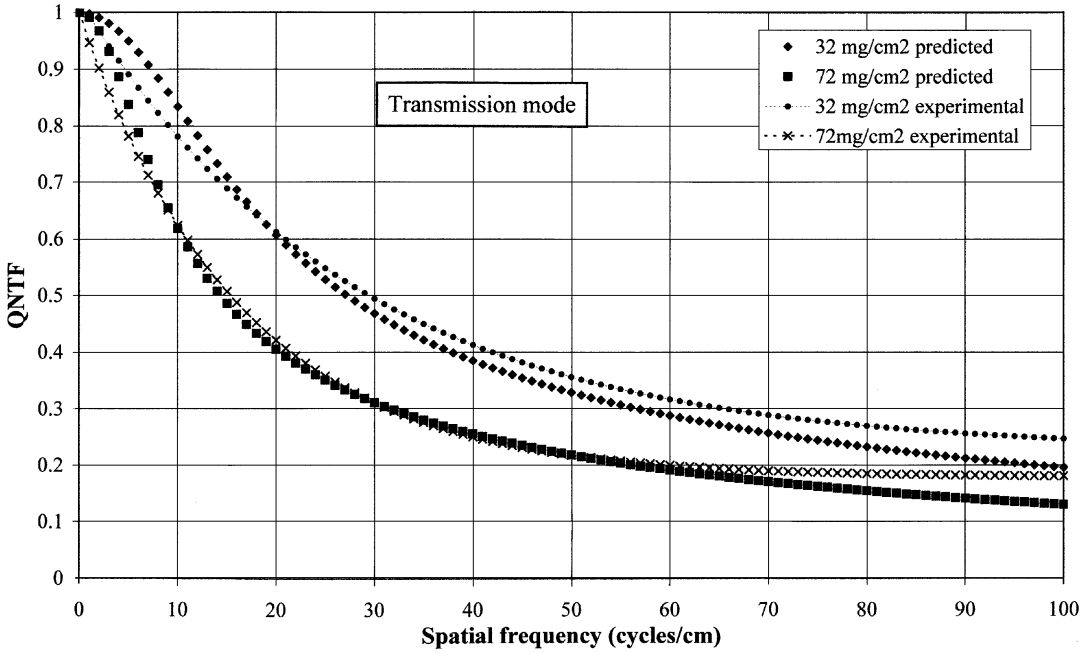

Fig. 3. Comparison between model predicted and experimental QNTF results for two Y_2O_3:Eu^{3+} phosphors, corresponding to coating thicknesses of 32 and 72 mg/cm^2, in transmission mode.

these conditions the effect of the K X-rays in energy absorption (3% of the total) is considered practically negligible [14].

Table 1 demonstrates how well the QNTF model matches experimental results for different values of σ. Furthermore, Table 1 provides an indication of the sensitivity of the model to σ.

A point worth commenting is that, under identical irradiation conditions, thin screens exhibit higher noise transfer functions than thicker ones. This may be explained by considering that QNTF is expressed as the weighted sum of the squares of the thin layers MTFs. These MTFs decrease with phosphor thickness increase, since the shape light bursts originating from depth t is broadened at thick phosphors. Therefore total screen QNTF is decreased. However, total screen QNTF decrease with thickness and frequency, is slower than the corresponding total screen MTF decrease, since the latter is expressed as a weighted sum of the MTFs of each thin layer [16,27].

Similarly, the presence of K X-rays reduces the thin layers MTFs since a fraction of the energy carried away by the K X-rays is reabsorbed in sites away from the site of the primary interaction. This in turn reduces total screen QNTF, which however decreases slower than MTF [3,16,27]. In all cases QNTF depends on the shape of light bursts, described by the Point Spread Function, which is affected by screen thickness [16]. As it is also

Table 1
The relative deviation, δ, of experimental and predicted theoretical QNTF results, for different values of σ is demonstrated. δ equals to the relative difference between the areas under the curves corresponding to experimental and predicted QNTF(u) results, expressed as a percentage

σ(cm^2/g)	δ(%)
15	− 10.568
20	− 4.280
25	− 1.597
26	0.698
30	4.970
35	8.841

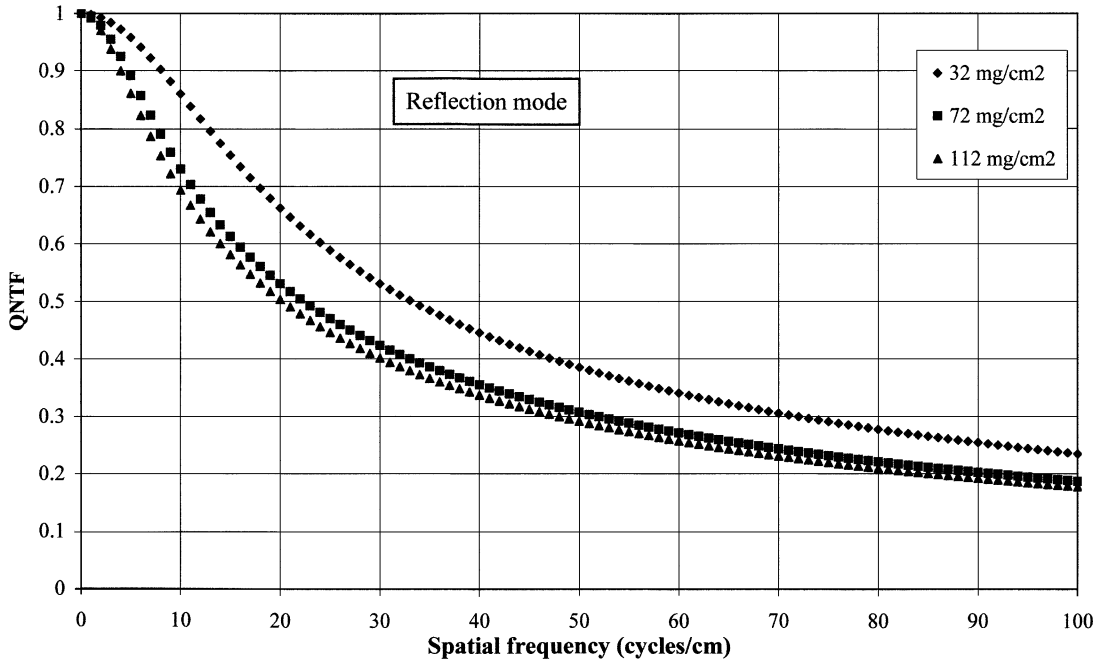

Fig. 4. Model predicted QNTF taking into account the K characteristics X-rays of three $Y_2O_3:Eu^{3+}$ phosphors, corresponding to coating thicknesses of 32, 72 and 112 mg/cm^2, in reflection mode.

observed from Fig. 4, QNTF differences between screens decrease as screen thickness increases. This effect is principally due to the X-ray absorption properties, which approximately follow the exponential law $(1 - \exp[\mu(E)t])$. Thus, as phosphor thickness increases the X-ray absorption differences between screens are minimized.

In Fig. 4 the results of a back screen configuration setup are shown. The form of the curves, as well as the QNTF variation with coating thickness are similar as to the front screen configuration setup. However, an increase of QNTF values for the same coating thickness as a function of frequency is observed. This can be justified by the fact that light yield mainly originates from low depths with respect to the irradiated screen surface. This is due to the exponential law of absorption, which imposes that X-ray energy is largely absorbed close to the surface. This induces better transfer characteristics [16], because of the lower light attenuation. Conclusively better signal and therefore noise transfer is accomplished.

4. Summary

This study presents an analytical model, which takes into consideration the effect of reabsorption of K characteristic X-rays and the optical properties of phosphor material, predicting the quantum noise power spectrum and subsequently the quantum noise transfer function of granular phosphor screens. The model shows good correlation with QNTF experimental data of $Y_2O_3:Eu^{3+}$ phosphors, within experimental accuracy. Additionally, the model describes in a satisfactory way the effect of phosphor thickness on quantum noise transfer properties of screens, as well as the differences between back screen and front screen configuration setup (irradiation geometry).

Acknowledgements

This study is dedicated to the memory of Prof. G.E. Giakoumakis, leading member of our team,

whose work on phosphor materials has inspired us to continue.

Appendix A

Let N photons of energy E be incident on a thin phosphor layer of thickness Δt. If the layer is infinitesimally thin, then the interaction of a photon in this layer can be treated as a binomial process, that is the photon will either interact or not. If p_i is the probability of interaction and q_i is the probability of non-interaction then $p_i = 1 - e^{-\mu_{tot}\Delta t}$ and $q_i = 1 - p_i$. The mean value of the interaction process is $u = Np$ and the variance is $\mathrm{var}(u) = Npq$.

Following the work of Rimcus and Baily [28] we implemented probability generating functions (PGF) to describe the binomial distribution. So in terms of PGF, the interaction process for realization over N photons can be described as [28]

$$\mathrm{PGF}_i = [F(s)]^N = [q_i + p_i(s)]^N, \tag{A.1}$$

where, index i stands for interaction. The photons that have interacted will either deposit energy in this layer or not. This process can be treated again as binomial process. If the probability of energy deposition is called p_a and the probability of non energy deposition is called q_a then [12,13]

$$p_a = \frac{\mu_{en}}{\mu_{tot}}(1 - e^{-\mu_{tot}\Delta t}) = ap_i \quad \text{and} \quad q_a = 1 - p_a, \tag{A.2}$$

where a is the ratio of the total energy mass absorption coefficient to total mass interaction coefficient [12,13].

The corresponding PGF_a over N trials equals

$$\mathrm{PGF}_a = [q_a + p_a(s)]^N = [g(s)]^N. \tag{A.3}$$

The joined PGF, $h(s)$, equals to $g(F(s))$ given by

$$h(s) = q_a + p_a[q_i + p_i(s)] = q_a + p_a q_i + p_a p_i(s). \tag{A.4}$$

By denoting $X = q_a + p_a q_i$ and $Y = p_a p_i$, then the process $[h(s)]^N = [X + Y(s)]^N$ is again a binomial process with mean value U and variance $\mathrm{var}(U)$ where

$$U = NY = Np_a p_i \quad \text{and}$$

$$\mathrm{var}(U) = NXY = N(q_a + p_a q_i)(p_a p_i). \tag{A.5}$$

By taking into account relations (A.2) and (A.4) one obtains:

$$\mathrm{var}(U) = N[1 - p_a + p_a(1 - p_i)](p_a p_i)$$

$$= N(1 - p_a p_i)(p_a p_i). \tag{A.6}$$

The second term of this product equals (due to (A.2), (A.4) and because Δt is considered infinitesimally thin) to

$$1 - p_a p_1 = 1 - ap_i^2 = 1 - \frac{\mu_{en}}{\mu_{tot}}(1 - e^{-\mu_{tot}\Delta t})^2$$

$$= 1 - \mu_{en}\mu_{tot}(\Delta t)^2 \cong 1. \tag{A.7}$$

Therefore, $\mathrm{var}(U) = Np_a p_i$ which holds for Poisson distribution. Thus, the process of energy deposition in the phosphor material can be satisfactorily described as a Poisson process.

References

[1] R.S. Holland, in: A.G. Haus (Ed.), The Physics of Medical Imaging: Recording System, Measurements and Techniques, American Association of Physicists in Medicine, New York, 1979, pp. 152–171.
[2] P.C. Bunch, K.E. Huff, R.J. Van Meter, J. Opt. Soc. Am. A 4 (1987) 902.
[3] R.M. Nishikawa, M.J. Yaffe, Med. Phys. 17 (1990) 887.
[4] J. Beutel, B.A. Apple, R. Shaw, Phys. Med. Biol. 38 (1993) 1181.
[5] L.W. Goldman, Med. Phys. 19 (1992) 45.
[6] R. M Nishikawa, M.J. Yaffe, Med. Phys. 17 (1990) 894.
[7] M. Drangova, J.A. Rowlands, Med. Phys. 15 (1988) 151.
[8] C. E Metz, C.J. Vyborny, Phys. Med. Biol. 28 (1983) 547.
[9] H.-P. Chan, K. Doi, Med. Phys. 11 (1984) 37.
[10] W. Hillen, W. Eckenbach, P. Quadflieg, T. Zaengel, Proc. SPIE 443 (1991) 120.
[11] J.A. Rowlands, K.W. Taylor, Med. Phys. 10 (1983) 786.
[12] H.P. Chan, K. Doi, Phys. Med. Biol. 28 (1983) 565.
[13] E. Storm, H. Israel, Report LA-3753 Los Alamos Scientific Laboratory of the University of California, 1967.
[14] D. Cavouras, I. Kandarakis, G. Panayiotakis, E. Evangelou, C. Nomicos, Med. Phys. 23 (1996) 1965.
[15] I. Kandarakis, D. Cavouras, G.S. Panayiotakis, C. Nomicos, Phys. Med. Biol. 42 (1997) 1351.

[16] R.M. Nishikawa, M.J. Yaffe, R.B. Holmes, Med. Phys. 16 (1989) 773.
[17] R.K. Swank, Appl. Opt. 12 (1973) 1865.
[18] G.W. Ludwig, J. Electrochem. Soc. 118 (1971) 1152.
[19] R.M. Nishikawa, M.J. Yaffe, Proc. SPIE 914 (1988) 128.
[20] C.E. Dick, J.W. Motz, Med. Phys. 8 (1981) 337.
[21] R.M. Nishikawa, M.J. Yaffe, Med. Phys. 12 (1985) 32.
[22] H. Kuhn, W. Knüpfer, Med. Phys. 19 (1992) 449.
[23] G.T. Barnes, D.P. Chakraborty, Radiology 145 (1982) 815.
[24] D.M. Tucker, G.T. Barnes, X. Wu, Med. Phys. 18 (1991) 402.
[25] J.R. Greening, in: Fundamentals of Radiation Dosimetry, 2nd ed., IOP, Bristol, UK, 1992, pp. 6–34.
[26] W.H. Press, B.P. Flannery, S.A. Teukolsky, W.T. Vetterling, in: Numerical Recipes in Pascal: The Art of scientific Computing, Cambridge University Press, Cambridge, 1989, pp. 575–580.
[27] G. Lubberts, J. Opt. Soc. Am. 58 (1968) 1475.
[28] D. Rimkus, N.A. Baily, Med. Phys. 10 (1984) 470.